A panel of four miRNAs (miR-190b, miR-584-5p, miR-452-5p, and miR-1306-5p) is capable of classifying luminal and non-luminal breast cancers.

Faranak Farahmand[1], Saied Rahmani[2,3], Hadi Bayat[1], Adel Salimi[2], Sogol Ghanbari[1], Ali Sharifi-Zarchi[2], Mohammad Vasei[4], Seyed-Javad Mowla[1,5*]

Affiliations:

1. Molecular Genetics Department, Biological Sciences Faculty, Tarbiat Modares University, Tehran, Iran
2. Computer Engineering Department, Sharif University of Technology, Tehran, Iran
3. Institute for Research in Fundamental Sciences (IPM), Tehran, Iran
4. Department of Pathology Shariati Hospital, Tehran University of Medical Sciences, Tehran, Iran
5. TechAzma Company, Tehran, Iran

* Corresponding author: Dr. Seyed Javad Mowla, Department of Molecular Genetics, Faculty of Biological Sciences, Tarbiat Modares University, Jalal AleAhmad, Nasr, Tehran, Iran. Tel.: +9821-82883464; Fax: +9821-82884717; E-mail: sjmowla@modares.ac.ir

Abstract.

BACKGROUND: Identifying the molecular subtypes of breast cancer (BC) plays a crucial role in enhancing the efficacy of therapy. MiRNAs with differential expressions in different subtypes of breast tumors can be considered non-invasive biomarkers for diagnosing BC subtypes.

OBJECTIVE: We aimed to investigate the efficacy of miR-190b, miR-584-5p, miR-452-5p, and miR-1306-5p as new potential diagnostic biomarkers in discriminating patients with luminal and non-luminal BCs.

METHODS: A group of miRNAs significantly associated with estrogen cell receptors (ER) in breast tumors was identified using feature selection methods analysis on miRNASeq data of TCGA and GSE68085. Among them, four miRNAs were selected as novel potential biomarkers, and their expression levels were assessed within luminal tumors, non-luminal tumors, and adjacent non-tumor tissues by qRT-PCR. Their impact on diagnosis was also evaluated by ROC curve analysis.

RESULTS: MiR-190b was remarkably up-regulated, while miRNA-584-5p, miRNA-452-5p, and miRNA-1306-5p were significantly down-regulated in luminal BCs. This group could discriminate luminal and non-luminal BCs at an AUC of 0.977.

CONCLUSIONS: According to our findings, these four miRNAs are promising biomarkers in parallel with histologic diagnosis methods for identifying patients who are most likely responding to specific therapies based on ER status.

Keywords: Breast Cancer (BC), Luminal BC, non-Luminal BC, Estrogen Receptors (ER), miRNAs, Biomarker

1 Introduction

Breast cancer (BC) has been the leading cause of cancer death (15.5%) and the most common cancer in females (24.5%) worldwide [1]. Despite significant improvements in the understanding of cancer pathogenesis and screening programs for early diagnosis and treatment over the past few decades, there are still about 2.2 million new cases of BCs with more than half a million BC-related deaths recorded annually worldwide [1]. BC has heterogeneous nature with various morphologic signs and clinical outcomes, which can be categorized in several aspects, including clinical features, expression of tumor markers, and histologic types [2, 3]. In this regard, gene expression profiles analysis has led to the classification of BCs based on hormone receptors, including estrogen receptor (ER), progesterone receptor (PR), and human epidermal growth factor receptor (HER2) status, which are crucial factors in therapeutic prediction and should be measured on all newly diagnosed BC tumors [4-7]. ER and PR mediate mammary cell proliferation signals and stimulate the growth of both normal and neoplastic breasts [8]. ERBB2, which is known as HER2 or HER2/neu, is a transmembrane receptor tyrosine kinase in the epidermal growth factor receptor family [8]. In line with these premises, in the early 2000s, the intrinsic molecular subtypes of BC were classified as luminal A (ER+/PR±/HER2–), luminal B (ER+/PR±/HER2+), HER2 enriched (ER–/PR–/HER2+), basal-like and normal-like, which show specific biological features and clinical outcomes [6].

The ER expression in BCs is frequently examined by immunohistochemistry on tumor tissues obtained by biopsy to separate BC subtypes in a clinical setting in predicting both prognosis and the likelihood of response to endocrine therapy [9]. However, the main disadvantage of this assay is false-negative results which contribute to patients being denied for hormone therapy based on erroneous test results. Diagnosis by tissue biopsy also is an invasive process which has the risk of

spreading tumor cells to adjacent tissues [10, 11]. Therefore, considering the limitations of common diagnostic tests, there is an essential need of developing new assays with high sensitivity and specificity for BC subtypes detection. In this regard, biomarkers are now investigated in cancer studies for the purpose of diagnosis, prognosis and therapy [12].

MiRNAs, which are small non-coding RNAs with 19–25 nucleotides, perform post-transcriptional regulation of gene expression by binding to the target mRNA and affecting many biological processes including differentiation, proliferation, apoptosis, and metastasis [13]. Dysregulated expression of miRNA play primary roles in cancer initiation, progression, and metastasis [12, 13]. During recent years, an increasing number of miRNAs acting either as important oncogenes or tumor suppressors in regulating BC initiation and progression have been investigated [14]. Due to remarkable stability and easily non-invasive detection of miRNAs in body fluids, such as serum and plasma, they are also considered as potential biomarkers in cancer diagnosis and prognosis [12, 15-18]. In this line, numerous studies have reported expression patterns of miRNAs as an informative tool for the classification of BCs [19, 20]. Although many studies have been done to discover biomarkers based on miRNAs, exploration of novel groups of miRNAs with high sensitivity and specificity for diagnosis of each subtype of BC, is valuable for development of diagnosis strategies, specific treatment and disease management. The main purpose of the present study was to identify promising miRNA biomarkers which are associated with the presence of ER in BCs. For this aim, we utilized boruta [21], XGBoost [22], and limma [23] R packages for TCGA and GEO data analysis, in addition to quantitative RT-PCR (qRT-PCR) method for experimental validation of the efficacy of our predicted miRNA biomarkers in discriminating luminal BCs from non-luminal BCs in 49 breast tumor specimens. Furthermore, we evaluated the role of these miRNAs as biomarkers for BC diagnosis by measuring their expression in breast tumor and non-

tumor samples of TCGA dataset and those samples used in the qRT-PCR analysis. Finally, we confirmed the efficacy of miR-190b as the potential biomarker of ER+ (luminal), and miRNA-584-5p, miRNA-452-5p, and miRNA-1306-5p as potential biomarkers of ER– (non-luminal) breast tumors.

2 Materials and methods

2.1. Analysis of miRNA-Seq datasets

Raw read counts of miRNAseq (miRseq) dataset of BC patients along with their clinical dataset from TCGA [24] were obtained and analyzed by TCGAbiolinks package [25]. The total number of samples in this dataset was 1175 (1072 tumor and 103 adjacent non-tumor samples). Intrinsic subtype labels were assigned to samples according to the expression level of ER, PR, and HER2 from IHC test results reported in clinical data. Datasets of BC subtypes based on cell receptors were presented in Positive/Negative format and level of existence format. In addition to TCGA, raw read counts of miRseq dataset of patients with TNBC and luminal BCs were obtained from GSE68085 [26].

In this research, we applied boruta feature selection, XGBoost feature selection, and limma differentially expression analysis on TCGA data and GSE68085 both of which contain miRseq data. Boruta is an R package utilizing a random forest model to classify data. The key idea of Brouta for selecting features is to permute each feature between samples and measure the significance of changes in model accuracy by a statistical test. We also used the XGBoost R package that provides a regression and classification model based on tree models and ensemble technique, which provides a method that assigns a score to each feature based on the location and number of features that appeared in internal nodes of the tree models. Further, we combined all

the results to reach the most generalizable miRNA biomarkers. We suppose that there are several miRNAs that are significantly associated with the existence of cell receptors, therefore, this association should be found in most of datasets and by the majority of methods without considering methods and experiment biases. The final result of a feature selection method on a dataset is an ordered list of miRNAs. To merge the results of different methods of feature selection on a dataset in a statistically acceptable manner, the Stuart method from the 'RobustRankAggreg' package in R was used. Also in the other cases that we need to merge multiple ordered lists we utilize the same strategy. After investigating miRNAs that are significantly associated with the existence of cell receptors in breast tumors, we used the ggplot2 R package to generate box plots by which we could evaluate the differential expressions of the top ten miRNAs with the highest association to ER between luminal and non-luminal breast tumor samples of miRseq datasets. We also reviewed the related previous studies to identify those miRNAs which have not been previously reported as biomarkers for BC subtypes. A group of miRNAs were then selected and ROC curves were generated using pROC package [27] to evaluate their specificity and sensitivity in distinguishing ER+ and ER– samples of miRseq datasets.

2.2. Patients and samples

A total of 85 BC specimens were retrieved from patients undergoing surgery, at Khatam-al-Anbia and Rasoul-Akram Hospitals, Tehran, Iran. This research involved collecting human tissues with no examination on human subjects. Tissue samples were categorized into 36 pairs of breast tumors and their adjacent non-tumor tissues plus 13 breast tumor samples from October 2018 to June 2019. All tumor samples were examined by pathologists and classified according to the standard histopathological parameters.

Tissue samples were immediately snap-frozen in liquid nitrogen after surgery and stored at -80°C until their RNA were extracted. Clinicopathological characteristics of patients are summarized in **Supplementary Table 1**. The research protocol for in vitro experiments on tissue samples was approved by the ethics committee of Ferdowsi University of Mashhad (code number: IR.UM.REC.1399.104).

2.3. RNA extraction

For isolating the Total RNA from breast tissues, RiboEx Total RNA reagent (GeneAll Biotechnology, South Korea) was used. The concentration of the extracted RNA was then quantified using a NanoDrop™ spectrophotometer. The purity of the RNA was validated via measuring the ratio of the absorbance at 260 and 280 nm. The quality of RNA which is regarded as the absence of degraded RNA was evaluated by agarose gel electrophoresis and ethidium bromide staining. Accordingly, the 18S and 28S RNA bands were visualized under ultraviolet light.

2.4. Polyadenylation and reverse transcription (cDNA synthesis)

Following RNA isolation, 1 μg of total RNA was poly-adenylated using Poly(A) Polymerase Tailing Kit (New England Biolabs., UK., Ltd.). Concisely, 10x reaction buffer (1 μl), 10 mM ATP (1 μl), Poly(A) polymerase (1 unit), and enough DEPC-treated water to make up 10 μL of solution were added to an RNAs free tube containing 1 μg total RNA. The solution was then incubated at 37°C for 30 min, followed by a 5 min incubation at 65°C for inactivating the enzyme. In the next step, the poly-adenylated RNA (10 μl) was converted to complementary DNA (cDNA) by adding Anchored Oligo(dT) (2 μl), 5X Reaction Buffer (4 μL), 10 mM dNTP Mix (2 μl), 1 μl of RevertAid

M-MuLV RT (200 U/µL) (Thermo Fisher Scientific., UK), and 1 µl of RiboLock RNase Inhibitor (20 U/µL). After a 10 minutes incubation at 25 °C and a 60 minutes incubation at 47 °C, the solution was heated at 85 °C for 5 minutes to stop the reaction, and it was kept at 4 °C until use.

2.5. Stem–loop RT–PCR

Stem-loop reverse transcription was performed for one of the candidate miRNAs using stem-loop primers. Reverse transcriptase reactions contained 1 µg of total RNA samples,1 µl of 1 pM stem-loop RT primer, 4 µl of 5X Reaction Buffer, 2 µl of 10 mM dNTP Mix, 1 µl of RiboLock RNase Inhibitor (20 U/µL), and 1 µl of RevertAid M-MuLV RT (200 U/µL) (Thermo Fisher Scientific., UK). After a 10 minutes incubation at 25 °C and a 60 minutes incubation at 47 °C, the solution was heated at 85 °C for 5 min to stop the reaction, and it was kept at 4 °C until use.

2.6. qRT-PCR

QRT-PCR was performed to quantitatively assess the expression of our selected miRNAs in tissue samples. Syber Green PCR Master Mix (BIOFACT Co., Ltd., Korea) and primers listed in **(Supplementary Tables 2 and 3)** were utilized for qRT-PCR which was conducted on a StepOne Plus System. The following PCR protocol was used: initial 10 minutes denaturation at 95°C, then 40 cycles at 95°C for 15 s, 60°C for 20 s, 72°C for 20 s. The mean delta Ct values of triplicate real-time qRT-PCR amplifications were utilized in statistical analysis. The comparative delta Ct values were used as the relative quantification of miRNAs, using the U48 small RNA [28-30] for normalization (deltaCt = CtmiRs-CtU48). $2^{-\Delta Ct}$ values were used to measure the expression levels of miRNAs in breast samples.

2.7. Primer validation

OligoAnalyzer 3.1 was employed to analyze the potential secondary structure and dimerization of primers. Melt curves with Single peaks were observed in qRT-PCR for the products of all primer pairs. To validate the amplified sequences, the accuracy of all PCR products was approved by cloning into T-vector and finally validated by golden standard sequencing method.

2.8. Statistical analysis

GraphPad Prism ver. 8 (GraphPad Software Inc., La Jolla, CA, USA) was applied for statistical analysis of the results obtained by qRT-PCR. The unpaired t-test, a two-tailed Mann-Whitney test, was used to compare the differential expression level of selected miRNAs within the luminal and non-luminal breast tumor samples.

The paired t-test was used for comparison of our selected miRNAs expression level between breast tumor and their adjacent non-tumor tissues. Results with p-value < 0.05 were considered as significant. Receiver operating characteristic (ROC) curves were also plotted by GraphPad Prism ver. 8 to validate the capability of the chosen miRNAs to distinguish between luminal and non-luminal tumor samples and between breast tumors and their adjacent non-tumor samples used in qRT-PCR. This was performed both individually and for a combination of all selected miRNAs. The area under curve (AUC) was also employed as an evaluation criteria for diagnostic performance of each miRNA and a combination of all miRNAs; the higher AUC, the better diagnostic performance (the AUCs closer to 1 reflect more substantial differences).

3 Results

3.1. Predicted ER associated miRNAs in breast tumors

The miRNAs with the highest possibility to be associated to ER were identified and ordered using limma, xgboost, bruta, and RobustRankAggreg' packages. As we aimed to investigate potential biomarkers of luminal and non-luminal breast tumors, we focused our study on the top ten most strongly ER associated miRNAs including miR-190b (MiR-190b is classified as miR-190b-3p and -5p in the latest version of miRBase Sequence Database (Release 22.1), Here, our candidate is miR-190b-5p.), miR-18a-5p, miR-505-3p, miR-224-5p, miR-577, miR-135b-5p, miR-584-5p, miR-452-5p, miR-452-3p, and miR-1306-5p **(Table 1)**. The expression status of these top ten miRNAs in BC were investigated in UCSC genome browser (GRCH37/hg19), and their differential expression were investigated in luminal and non-luminal breast tumor samples of TCGA **(Supplementary Fig. 1)**. We excluded miR-577 and miR-452-3p from the top ten list due to their extremely low expression levels in breast tumors. The first rank miR-190b with the highest score in the list was selected as the potential biomarker of ER+ breast tumors. The expression levels and the association of miR-18a-5p [31], miR-505-3p [32], miR-224-5p [33, 34], and miR-135b-5p [35] with ER have been previously investigated in breast cancer. Therefore, we excluded miR-18a-5p, miR-505-3p, miR-224-5p, and miR-135b-5p from the study, and we selected those miRNAs which association to highly aggressive breast tumors (ER–) have not been previously studied including miR-584-5p, miR-452-5p, and miR-1306-5p to evaluate their potential as biomarkers of ER– breast tumors.

Table 1. Top-ranked most strongly ER associated miRNAs.

ER	Aggregate Score
miR-190b	0.000032
miR-18a-5p	0.000256
miR-505-3p	0.002304
miR-224-5p	0.00484
miR-577	0.005816
miR-135b-5p	0.007
miR-584-5p	0.01024
miR-452-5p	0.065408
miR-452-3p	0.075656
miR-1306-5p	0.114264

The results of the RobustRankAggreg package analysis of miRseq datasets are summarized in this table. MiRNAs with a lower aggregate score are associated to ER receptors with a higher probability. Our candidate miRNAs are in bold style.

3.2. Evaluation of miR-190b expression in luminal compared to non-luminal breast tumors

The higher expression level of miR-190b in luminal compared to non-luminal breast tumors, which was identified previously by analyzing the available miRseq data in TCGA **(Fig. 1B and 1C)** and GSE68085 **(Fig. 1D)** datasets, was validated experimentally by qRT-PCR **(Fig. 1A)**. Indeed, we found a similar significant higher expression level of miR-190b in 24 luminal compared to 23 non-luminal breast tumor samples ($P < 0.05$). Moreover, as shown in **Fig. 1C**, the expression level of miR-190b correlates positively with the percentage of ER level in breast tumor cells, which indicates that the higher the ER level is, the more miR-190b is expressed in breast tumors.

Fig. 1: The expression level of miR-190b in patients with luminal compared to non-luminal BCs. A) The results of qRT-PCR analysis show that the expression level of miR-190b (relative to u-48) in luminal breast samples is significantly higher than non-luminal breast samples (P.value < 0.05). **B)** The results of bioinformatics analysis of miRseq dataset of BC patients in TCGA also show a significant up-regulation of miR-190b in luminal versus HER2 and TNBC (non-luminal) breast tumor samples (P.value < 0.05). **C)** The results of bioinformatics analysis of miR-190b expression level based on the percentage of ER level indicate a positive correlation between miR-190b and ER expression level. **D)** The results of bioinformatics analysis of the GSE68085 dataset also represent a significant higher expression of miR-190b in luminal compared to TNBC breast tumor samples (P.value < 0.05).

3.3. Evaluation of the expression levels of miR-584-5p, miR-452-5p, and miR-1306-5p in luminal compared to non-luminal breast tumors

The expression levels of miR-584-5p, miR-452-5p, and miR-1306-5p selected in miRseq analysis were then assessed in breast tumor samples by qRT-PCR **(Fig. 2A)**. Accordingly, we validated the significant down-regulation of these miRNAs in luminal compared to non-luminal breast tumors which was predicted previously by analyzing the available miRseq data in TCGA **(Fig. 2B** and **2C)** and GSE68085 **(Fig. 2D)** datasets (P < 0.05). **Fig. 2C** also demonstrates a negative correlation between the percentage of ER level and the expression levels of miR-584-5p, miR-452-5p, and miR-1306-5p in breast tumors.

Overall, the results obtained by qRT-PCR confirmed the data observed in the miRseq analysis.

Fig. 2: The expression level of miR-584-5p, miR-452-5p, and miR-1306-5p in patients with luminal compared to non-luminal BCs. A) The results of qRT-PCR analysis show that the expression level of miR-584-5p, miR-452-5p, and miR-1306-5p (relative to u-48) in luminal breast samples is significantly lower than non-luminal breast samples (P.value < 0.05). **B)** The results of bioinformatics analysis of miRseq dataset of BC patients in TCGA also show down-regulation of miR-584-5p, miR-452-5p, and miR-1306-5p (P.value < 0.05) in luminal versus HER2 and

TNBC (non-luminal) breast tumor samples. **C)** The results of miRseq analysis of miR-584-5p, miR-452-5p, and miR-1306-5p expression levels based on the percentage of ER level indicate a significant negative correlation between these three miRNAs and ER expression level (P.value < 0.05). **D)** The results of miRseq analysis of GSE68085 dataset also represent lower expression of miR-584-5p (P.value < 0.05), miR-452-5p, and miR-1306-5p in luminal compared to TNBC breast tumor samples.

3.4. Differential expression of our four selected miRNAs between breast tumor and non-tumor samples

At first, we identified expression profiles of our selected miRNAs between breast tumor and non-tumor samples (adjacent non-tumor breast tissues) in TCGA data using bioinformatics tools. We then evaluated their expression levels experimentally in 36 breast tumor cases and their adjacent non-tumor tissues by qRT-PCR analysis. Although, in miRseq analysis, miR-190b showed a significant increase in its expression in breast tumors compared to non-tumor breast samples **(Fig. 3A)**, the qRT-PCR analysis showed an overall decrease in the expression level of miR-190b in tumor tissues versus non-tumor adjacent tissues **(Fig. 3B)**. In further analysis, we found that the down-regulation of miR-190b in breast tumors was specific to ER−/PR− tumors since ER+/PR+ and ER+/PR− tumors showed a miR-190b up-regulation compared to non-tumor breast tissues **(Fig. 3C).**

Fig. 3: The expression level of miR-190b (relative to U-48) in breast tumor samples compared to non-tumor adjacent tissues. A) The results of miRseq analysis show a significant increase of miR-190b expression in breast tumors compared to non-tumor breast samples (P.value < 0.05). **B)** However, the results of qRT-PCR analysis show an overall decrease of miR-190b expression level in tumor tissues versus non-tumor adjacent tissues. **C)** The expression level of miR-190b in ER+ breast tumors is up-regulated compared to non-tumor adjacent tissues, whereas, in ER− breast tumors is down-regulated.

Fig. 4A, **B**, **D**, and **E** demonstrate the lower expression levels of miR-584-5p and miR-452-5p in breast tumor samples (both luminal and non-luminal) compared to non-tumor breast tissues based on both miRseq and qRT-PCR analysis. Although, in miRseq analysis, miR-1306-5p didn't show significant differential expression between breast tumor and non-tumor adjacent samples **(Fig. 4C)**, in qRT-PCR analysis it was significantly down-regulated in breast tumor tissues compared to their adjacent non-tumor tissues (p-value < 0.05) **(Fig. 4F)**.

Fig. 4: The expression level of miR-584-5p, miR-452-5p, and miR-1306-5p (relative to U-48) in breast tumor samples compared to non-tumor adjacent tissues. The results of miRseq analysis show that the expression levels of miR-584-5p **(A)**, and miR-452-5p **(B)** are significantly lower in breast tumors, as compared with non-tumor breast samples (P.value < 0.05), while the expression level of miR-1306-5p **(C)** shows no difference between breast tumors and non-tumor breast samples. The results of the qRT-PCR analysis show significant down-regulation of miR-584-5p **(D)**, miR-452-5p **(E)**, and miR-1306-5p **(F)** in tumor tissues versus non-tumor adjacent tissues (P.value < 0.05).

3.5. Roc Curve analysis

Each of the four candidate miRNAs, miR-190b, miR-584-5p, miR-452-5p and miR-1306-5p, showed high AUCs with values of 0.920 (specificity of 92%, and sensitivity of 83%), 0.846 (specificity of 80%, and sensitivity of 75%), 0.829 (specificity of 71%, and sensitivity of 84%), and 0.795 (specificity of 78%, and sensitivity of 70%), respectively **(Fig. 5A, B, C, and D)**. Interestingly, the AUC of the combination of miR-190b, miR-584-5p, miR-452-5p, and miR-1306-5p increased to 0.977 with the specificity of 93% and sensitivity of 96% in discriminating luminal and non-luminal samples of TCGA dataset **(Fig. 5E)**. A ROC curve was also plotted for the combination of miR-190b, miR-18a-5p, miR-505-3p, miR-224-5p, miR-135b-5p, miR-584-

5p, miR-452-5p, and miR-1306-5p which creates the similar AUC value of 0.977 **(Supplementary Fig. 2)**. Therefore, the addition of miR-18a-5p, miR-505-3p, miR-224-5p, and miR-135b-5p did not improve the AUC achieved by the combination of our selected miRNAs. In addition to the ROC curves obtained by miR-seq analysis, the GraphPad Prism was used to evaluate the diagnostic value of our selected miRNAs in discriminating luminal from non-luminal tissue samples used in qRT-PCR analysis. In concordance with AUCs obtained for miRNA levels in miRseq datasets, significant AUCs of 0.6938 (Specificity of 61%, and sensitivity of 75%), 0.6739 (Specificity of 60%, and sensitivity of 69%), 0.7773 (Specificity of 69%, and sensitivity of 87%), and 0.6656 (Specificity of 52%, and sensitivity of 77%) have been obtained for miR-190b **(Fig. 5F)**, miR-584-5p **(Fig. 5G)**, miR-452-5p **(Fig. 5H)**, and miR-1306-5p **(Fig. 5I)** respectively ($P<0.05$).

Fig. 5: The AUCs of ROC curves for miRNA levels in luminal and non-luminal samples. The capabilities of miR-190b **(A** and **F)**, miR-584-5p **(B** and **G)**, miR-452-5p **(C** and **H)**, miR-1306-5p **(D** and **I)**, and the combination of these four miRNAs **(E)** to discriminate luminal and non-luminal samples of TCGA **(A**, **B**, **C**, **D**, and **E)** and qRT-PCR analysis **(F**, **G**, **H**, and **I)** are shown in ROC curves.

As shown in the qRT-PCR results, miR-190b was up-regulated in ER+ breast tumors, whereas it was down-regulated in ER- tumors compared to non-tumor tissues. Therefore, we excluded this miRNA from the group of biomarkers which potency was evaluated in detection of breast tumors. Accordingly, ROC curves were plotted for miR-584-5p, miR-452-5p, and miR-1306-5p which represented the AUCs of 0.949 (specificity of 85%, and sensitivity of 95%), 0.867 (specificity of 98%, and sensitivity of 75%), and 0.635 (specificity of 42%, and sensitivity of 82%) in samples of miRseq analysis (**Fig. 6A, B, and C**), and the AUCs of 0.7662 (specificity of 64%, and

sensitivity of 78%), 0.6656 (specificity of 68%, and sensitivity of 60%), and 0.7052 (specificity of 61%, and sensitivity of 75%) in samples of qRT-PCR analysis **(Fig. 6F, G, and H)**.

Furthermore, **Fig. 6D** and **E** demonstrated that the combination of miR-584-5p and miR-452-5p yielded higher AUC value of 0.967 (specificity of 100% and sensitivity of 87%) compared to the combination of miR-584-5p, miR-452-5p, and miR-1306-5p which generated a ROC Curve with AUC value of 0.946 (specificity of 98% and sensitivity of 94%).

Fig. 6: The AUCs of ROC curves for miRNA levels in tumor and non-tumor samples. The potential of miR-584-5p **(A** and **F)**, miR-452-5p **(B** and **G)**, miR-1306-5p **(C** and **H)**, the combination of miR-584-5p and miR-452-5p **(D)**, and the combination of all these three miRNAs **(E)** to discriminate tumor and non-tumor samples of TCGA **(A, B, C, D, E)** and qRT-PCR analysis **(F, G, H)** are shown in ROC curves.

4 Discussion

Currently, Mammography is the gold standard tool for screening and diagnosis of breast cancer (BC). However, invasive histological evaluation of breast biopsy is required for accurate diagnosis of BC subtype. The identification of novel reliable minimally invasive BC biomarkers with high sensitivity and specificity would lead to a significant improvement in the clinical management of this complex disease [36]. Numerous studies have reported the significant role of miRNAs in the initiation and progression of BC and revealed that certain miRNAs are differentially expressed between different breast tumor subtypes. [37]. However, since they merely investigated differentially expressed miRNAs, in the current study we aimed to identify ER associated miRNAs to reach promising biomarkers. Therefore, we used the available data from TCGA and applied boruta and XGBoost feature selection and limma differentially expression analysis to obtain miRNAs that are significantly associated with the existence of cell receptors in breast tumors. As

a result, we reported herein the discovery of four miRNAs, miR-190b, miR-584-5p, miR-452-5p, and miR-1306-5p which are significantly associated with ER status in breast tumors, as predicted by *in silico* analysis. We then confirmed the efficacy of this signature in discriminating luminal BCs (ER+) and non-luminal BCs (ER–) by qRT-PCR.

Few studies, previously, have investigated the implications of miR-190b expression in BC. In this regard, it has been reported that miR-190b is associated with ER+ breast tumors [38] and resistance to hormone therapy [39]. It has been also previously identified by Cizeron-Clairac et al. 2015 as the highest upregulated miRNA in luminal compared to non-luminal tumors. In consistent with previous studies, our results also demonstrated the significant higher expression level of miR-190b in ER+ compared to ER– breast tumors ($P<0.05$). Moreover, ROC curve analysis showed the potential diagnostic value of miR-190b as a very interesting biomarker in distinguishing ER+ from ER– breast tumors with specificity of 92% and sensitivity of 83% (based on miRseq analysis). In another study, expression level of miR-190b was examined in seven BC cell lines and suggested that the biological and clinical implication of miR-190b may differ among BC subtypes [40]. Moreover, de Anda-Jáuregui et al. showed the up-regulation of miR-190b in ER+ breast tumors compared to normal breast tissues, whereas the down-regulation of miR-190b in ER– tumors compared to healthy controls [38]. In the present study, our in silico analysis represented an overall up-regulation of miR-190b in breast tumors versus adjacent non-tumor tissue. While, in the practical experiment, we observed the up-regulation of miR-190b in ER+ but not in ER– breast tumors. Hence, it should be noted that, the up-regulation of miR-190b in breast tumor samples versus non-tumor adjacent tissues was restricted to ER+ tumors. This discrepancy between the results of miRseq analysis and qRT-PCR analysis may be related to the higher number of ER+ tumors compared to ER– tumors in the TCGA dataset.

Previous studies mostly have focused on the role of miR-584-5p in lung cancer progression and metastasis [41-43]. The chromosomal region where miR-584 is located, 5q32, has been highlighted to be deleted in myelodysplastic syndromes that lead to malignant transformation [44, 45]. In addition, a study indicated that miR-584 may act as a tumor suppressor in renal carcinoma cells [46]. Furthermore, it was revealed that miR-584 is significantly down-regulated in human HER2+ breast tumors compared to non-tumor adjacent tissues [47]. Our results also showed significant down-regulation of miR-584-5p in breast tumors compared to adjacent non-tumor tissues, which may indicate the tumor suppressive role of miR-584-5p. According to ROC curve analysis, miR-584-5p also can act as a strong biomarker for BC diagnosis with high sensitivity and specificity (AUC of 0.949 in miRseq analysis and AUC of 0.7662 in qRT-PCR analysis). Additionally, our findings validated down-regulation of miR-584-5p in ER+ versus ER– breast tumors predicted by *in silico* analysis, and the AUC values of 0.846 and 0.6739 obtained by miRseq and qRT-PCR analysis, represented the notable capability of miR-584-5p in distinguishing non-luminal and luminal BC subtypes.

It is reported that miR-452 is abnormally expressed in different types of human cancer [48-50]. The down-regulation of miR-452 in BC tissues compared with paired normal breast tissues was also identified previously [51]. Moreover, miR-452 has been predicted to have an important role in regulation of pathways specific to luminal-A by TCGA data analysis [52]. In the present study, we also demonstrated the down-regulation of miR-452-5p in breast tumors versus adjacent non-tumor tissues. More importantly, for the first time, we showed that miR-452-5p can serve as a potential biomarker for distinguishing ER– from ER+ breast tumors with high sensitivity and specificity (AUC values of 0.829 and 0.7773 in miRseq and qRT-PCR analysis, respectively).

Although, until 2019, miR-1306-5p has not been reported to be enrolled in any cancers, aberrant expression of this miRNA in plasma samples of patients with different diseases such as heart failure, glaucoma, or epilepsy has been detected [53]. Recently, miR-1306 has been reported to be aberrantly expressed in some types of human cancers including breast and colorectal cancers [53, 54]. In this regards, the up-regulation of miR-1306-5p was observed in subjects with malignant breast lesions compared to benign tumors [53]. The present study also represented the up-regulation of miR-1306-5p in ER– breast tumors which typically are more aggressive than ER+ tumors. However, the down-regulation of miR-1306-5p in breast tumors compared to non-tumor adjacent tissues may suggest its tumor suppressive role. This discrepancy needs to be elucidated in future studies as the role of this miRNA has not been widely characterized in BC. Likewise, no previous study have been performed to investigate the expression level and biological roles of miR-1306-5p in BC subtypes. Hence, this is the first study which reveals the efficacy of miR-1306-5p in distinguishing ER+ and ER– breast tumors with AUC values of 0.795 and 0.6656 based on *in silico* and qRT-PCR analysis, respectively.

Overall, the AUCs acquired by qRT-PCR were not as high as those of miR-seq analysis (except for miR-1306-5p level in tumor and non-tumor samples). This discrepancy could be attributed to the much higher number of breast tumor samples used in miRseq analysis compared to the samples used in qRT-PCR. For identifying the best biomarker panel, we compared the AUCs produced from ROC curve analysis for each individual miRNA and miRNA combination profiles in distinguishing luminal and non-luminal BC samples of TCGA, which revealed that the best AUC of 0.977 was generated from a combination of miR-190b, miR-584-5p, miR-452-5p, and miR-1306-5p, providing a specificity of 93% and sensitivity of 96%.

Furthuremore, the ROC curve for the combination of the two differentially expressed miRNAs, miR-584-5p, and miR-452-5p in breast tumors and non-tumor samples of TCGA, showed an extremely high diagnostic accuracy with an AUC value of 0.967 with specificity of 100% and sensitivity of 87%. It should be noted that miR-190b was not included in this biomarker set because its differential expression in breast tumors compared to non-tumor tissues depends on the tumor subtype. The ROC curve of the combination of miR-584-5p, miR-452-5p, miR-1306-5p also creates the AUC of 0.946. Therefore, the addition of miR-1306-5p did not improve the AUC achieved. Although the signature of miR-584-5p and miR-452-5p is an effective diagnostic test alone with a strong performance (specificity of 100% and sensitivity of 87%), it may show promise as a valuable assessment tool in BC diagnosis in combination with screening mammography.

A particular strength of this study is that the reported miRNA panel consists of four miRNAs, as such panels are likely less prone to biological differences than single miRNAs so these panels are more reliable for clinical use. A second strength is that the measured expression level of our four miRNA signature in breast tumor samples revealed a specific algorithm which help to detect the ER status of each sample. To clarify, in ER+ tumors the expression level of miR-190b was higher than that of miR-584-5p, miR-452-5p, and miR-1306-5p, while, in ER– tumors miR-190b expression level was lower than that of these three miRNAs **(Supplementary Fig. 3)**. However, since the miR-452-5p expression level was not detectable in a number of tumor samples, the role of miR-452-5p in this algorithm needs further investigations.

5 Conclusion

Overall, our study signifies the discovery of a four-miRNA (miR-190b, miR-584-5p, miR-452-5p, and miR-1306-5p) panel, which expression is associated to ER in breast tumors, as a novel

biomarker for diagnosis of luminal and non-luminal BC subtypes. Based on this miRNA panel, we have represented a classification model with high discrimination ability in classifying luminal and non-luminal BCs at an AUC of 0.977. In addition, the panel containing miR-584-5p, and miR-452-5p is shown to have the efficacy to be developed as a parallel test to examine breast samples of patients with abnormal screening mammograms, with the aim of reducing false-positive results. For future investigations, these two miRNA signatures should be evaluated in blood serum samples to confirm the clinical utility of these miRNA signatures.

Acknowledgments

Not applicable.

Author contributions

Conception: Faranak Farahmand

Interpretation or analysis of data: Faranak Farahmand, Saeid Rahmani, Hadi Bayat

Preparation of the manuscript: Faranak Farahmand, Saeid Rahmani

Revision for important intellectual content: Faranak Farahmand, Saeid Rahmani, Seyed-Javad Mowla, Hadi Bayat, Adel Salimi, Sogol Ghanbari, Ali Sharifi-Zarchi, Mohammad Vasei

Supervision: Seyed-Javad Mowla

Uncategorized References

1. Sung, H., et al., *Global cancer statistics 2020: GLOBOCAN estimates of incidence and mortality worldwide for 36 cancers in 185 countries.* CA: a cancer journal for clinicians, 2021. **71**(3): p. 209-249.
2. Coleman, W.B. and C.K. Anders, *Discerning clinical responses in breast Cancer based on molecular signatures.* The American journal of pathology, 2017. **187**(10): p. 2199-2207.
3. Li, C., D. Uribe, and J. Daling, *Clinical characteristics of different histologic types of breast cancer.* British journal of cancer, 2005. **93**(9): p. 1046-1052.
4. Hu, Z., et al., *The molecular portraits of breast tumors are conserved across microarray platforms.* BMC genomics, 2006. **7**(1): p. 1-12.
5. Chen, Y.-J., et al., *Molecular subtyping of breast cancer intrinsic taxonomy with oligonucleotide microarray and NanoString nCounter.* Bioscience reports, 2021. **41**(8).
6. Perou, C.M., et al., *Molecular portraits of human breast tumours.* nature, 2000. **406**(6797): p. 747-752.
7. Song, N., et al., *Prediction of breast cancer survival using clinical and genetic markers by tumor subtypes.* PLoS One, 2015. **10**(4): p. e0122413.
8. Joshi, H. and M.F. Press, *Molecular oncology of breast cancer*, in *The Breast*. 2018, Elsevier. p. 282-307. e5.
9. Hironaka-Mitsuhashi, A., et al., *A tissue microRNA signature that predicts the prognosis of breast cancer in young women.* PLoS One, 2017. **12**(11): p. e0187638.
10. Jorns, J.M., *Breast cancer biomarkers: challenges in routine estrogen receptor, progesterone receptor, and HER2/neu evaluation.* Archives of Pathology & Laboratory Medicine, 2019. **143**(12): p. 1444-1449.
11. Alba-Bernal, A., et al., *Challenges and achievements of liquid biopsy technologies employed in early breast cancer.* EBioMedicine, 2020. **62**: p. 103100.
12. Adhami, M., et al., *Candidate miRNAs in human breast cancer biomarkers: a systematic review.* Breast Cancer, 2018. **25**(2): p. 198-205.
13. Stahlhut, C. and F.J. Slack, *MicroRNAs and the cancer phenotype: profiling, signatures and clinical implications.* Genome medicine, 2013. **5**(12): p. 1-12.
14. Mu, H., et al., *miRNAs as potential markers for breast cancer and regulators of tumorigenesis and progression.* International Journal of Oncology, 2021. **58**(5): p. 1-12.
15. Arun, R.P., H.F. Cahill, and P. Marcato, *Breast Cancer Subtype-Specific miRNAs: Networks, Impacts, and the Potential for Intervention.* Biomedicines, 2022. **10**(3): p. 651.
16. Gupta, I., et al., *Circulating miRNAs in HER2-positive and triple negative breast cancers: potential biomarkers and therapeutic targets.* International Journal of Molecular Sciences, 2020. **21**(18): p. 6750.
17. Zhang, Y., et al., *Multilayer network analysis of miRNA and protein expression profiles in breast cancer patients.* PloS one, 2019. **14**(4): p. e0202311.
18. Schrauder, M.G., et al., *Circulating micro-RNAs as potential blood-based markers for early stage breast cancer detection.* PloS one, 2012. **7**(1): p. e29770.
19. Kudela, E., et al., *miRNA expression profiles in luminal A breast cancer—implications in biology, prognosis, and prediction of response to hormonal treatment.* International Journal of Molecular Sciences, 2020. **21**(20): p. 7691.

20. Dvinge, H., et al., *The shaping and functional consequences of the microRNA landscape in breast cancer.* Nature, 2013. **497**(7449): p. 378-382.
21. Kursa, M.B. and W.R. Rudnicki, *Feature selection with the Boruta package.* J Stat Softw, 2010. **36**(11): p. 1-13.
22. Chen, T., et al., *xgboost: Extreme Gradient Boosting (2017).* R package version 0.6-4, 2015.
23. Ritchie, M.E., et al., *limma powers differential expression analyses for RNA-sequencing and microarray studies.* Nucleic acids research, 2015. **43**(7): p. e47-e47.
24. Chang, K., et al., *The cancer genome atlas pan-cancer analysis project.* Nat Genet, 2013. **45**(10): p. 1113-1120.
25. Colaprico, A., et al., *TCGAbiolinks: an R/Bioconductor package for integrative analysis of TCGA data.* Nucleic acids research, 2016. **44**(8): p. e71-e71.
26. Krishnan, P., et al., *Next generation sequencing profiling identifies miR-574-3p and miR-660-5p as potential novel prognostic markers for breast cancer.* BMC genomics, 2015. **16**(1): p. 1-17.
27. Robin, X., et al., *pROC: an open-source package for R and S+ to analyze and compare ROC curves.* BMC bioinformatics, 2011. **12**(1): p. 1-8.
28. Xiang, M., et al., *U6 is not a suitable endogenous control for the quantification of circulating microRNAs.* Biochemical and biophysical research communications, 2014. **454**(1): p. 210-214.
29. Hirschberger, S., et al., *Identification of suitable controls for miRNA quantification in T-cells and whole blood cells in sepsis.* Scientific reports, 2019. **9**(1): p. 1-13.
30. Carvalho, T.M., et al., *MicroRNAs miR-142-5p, miR-150-5p, miR-320a-3p, and miR-4433b-5p in Serum and Tissue: Potential Biomarkers in Sporadic Breast Cancer.* Frontiers in Genetics, 2022: p. 1414.
31. Calvano Filho, C.M.C., et al., *Triple-negative and luminal A breast tumors: differential expression of miR-18a-5p, miR-17-5p, and miR-20a-5p.* Tumor Biology, 2014. **35**(8): p. 7733-7741.
32. Jonsdottir, K., et al., *Validation of expression patterns for nine miRNAs in 204 lymph-node negative breast cancers.* PloS one, 2012. **7**(11): p. e48692.
33. Zhang, L., et al., *MicroRNA-224 promotes tumorigenesis through downregulation of caspase-9 in triple-negative breast cancer.* Disease markers, 2019. **2019**.
34. Huang, L., et al., *MicroRNA-224 targets RKIP to control cell invasion and expression of metastasis genes in human breast cancer cells.* Biochemical and biophysical research communications, 2012. **425**(2): p. 127-133.
35. Aakula, A., et al., *MicroRNA-135b regulates ERα, AR and HIF1AN and affects breast and prostate cancer cell growth.* Molecular oncology, 2015. **9**(7): p. 1287-1300.
36. Fisher, B., C.K. Redmond, and E.R. Fisher, *Evolution of knowledge related to breast cancer heterogeneity: a 25-year retrospective.* Journal of Clinical Oncology, 2008. **26**(13): p. 2068-2071.
37. Blenkiron, C., et al., *MicroRNA expression profiling of human breast cancer identifies new markers of tumor subtype.* Genome biology, 2007. **8**(10): p. 1-16.
38. Cizeron-Clairac, G., et al., *MiR-190b, the highest up-regulated miRNA in ERα-positive compared to ERα-negative breast tumors, a new biomarker in breast cancers?* BMC cancer, 2015. **15**(1): p. 1-14.

39. Joshi, T., et al., *Integrative analysis of miRNA and gene expression reveals regulatory networks in tamoxifen-resistant breast cancer.* Oncotarget, 2016. **7**(35): p. 57239.
40. Dai, W., et al., *miR-148b-3p, miR-190b, and miR-429 regulate cell progression and act as potential biomarkers for breast cancer.* Journal of breast cancer, 2019. **22**(2): p. 219-236.
41. Ma, D., et al., *Circular RNA ABCB10 promotes non-small cell lung cancer progression by increasing E2F5 expression through sponging miR-584-5p.* Cell Cycle, 2020. **19**(13): p. 1611-1620.
42. Lee, S.B., et al., *Tumor suppressor miR-584-5p inhibits migration and invasion in smoking related non-small cell lung cancer cells by targeting YKT6.* Cancers, 2021. **13**(5): p. 1159.
43. Guo, T., et al., *miR-584-5p regulates migration and invasion in non-small cell lung cancer cell lines through regulation of MMP-14.* Molecular Medicine Reports, 2019. **19**(3): p. 1747-1752.
44. Eisenmann, K., et al., *5q–myelodysplastic syndromes: chromosome 5q genes direct a tumor-suppression network sensing actin dynamics.* Oncogene, 2009. **28**(39): p. 3429-3441.
45. Lehmann, S., et al., *Common deleted genes in the 5q− syndrome: thrombocytopenia and reduced erythroid colony formation in SPARC null mice.* Leukemia, 2007. **21**(9): p. 1931-1936.
46. Ueno, K., et al., *Tumour suppressor microRNA-584 directly targets oncogene Rock-1 and decreases invasion ability in human clear cell renal cell carcinoma.* British journal of cancer, 2011. **104**(2): p. 308-315.
47. Cava, C., et al., *Theranostic application of miR-429 in HER2+ breast cancer.* Theranostics, 2020. **10**(1): p. 50.
48. He, Z., et al., *Up-regulation of MiR-452 inhibits metastasis of non-small cell lung cancer by regulating BMI1.* Cellular Physiology and Biochemistry, 2015. **37**(1): p. 387-398.
49. Kristensen, H., et al., *Hypermethylation of the GABRE∼miR-452∼miR-224 promoter in prostate cancer predicts biochemical recurrence after radical prostatectomy.* Clinical Cancer Research, 2014. **20**(8): p. 2169-2181.
50. Liu, L., et al., *Downregulation of miR-452 promotes stem-like traits and tumorigenicity of gliomas.* Clinical Cancer Research, 2013. **19**(13): p. 3429-3438.
51. Li, W., et al., *Tumor-suppressive microRNA-452 inhibits migration and invasion of breast cancer cells by directly targeting RAB11A.* Oncology Letters, 2017. **14**(2): p. 2559-2565.
52. Cava, C., et al., *How interacting pathways are regulated by miRNAs in breast cancer subtypes.* BMC bioinformatics, 2016. **17**(12): p. 111-133.
53. Loke, S.Y., et al., *A circulating miRNA signature for stratification of breast lesions among women with abnormal screening mammograms.* Cancers, 2019. **11**(12): p. 1872.
54. Chang, N., et al., *Long Noncoding RNA LINC00857 Promotes Proliferation, Migration, and Invasion of Colorectal Cancer Cell through miR-1306/Vimentin Axis.* Computational and Mathematical Methods in Medicine, 2021. **2021**.

Supporting information captions:

Supplementary Fig. 1: The differential expression levels of miR-190b-5p **(A)**, miR-18a-5p **(B)**, miR-505-3p **(C)**, miR-224-5p **(D)**, miR-577 **(E)**, miR-135b-5p **(F)**, miR-584-5p **(G)**, miR-452-5p **(H)**, miR-452-3p **(I)**, and miR-1306-5p **(J)** in luminal versus non-luminal breast tumor samples of TCGA.

Supplementary Fig. 2: A ROC curve for the combination of miR-190b, miR-18a-5p, miR-505-3p, miR-224-5p, miR-135b-5p, miR-584-5p, miR-452-5p, and miR-1306-5p in luminal and non-luminal breast tumor samples of TCGA which created the AUC value of 0.977 with specificity of 95% and sensitivity of 93%.

Supplementary Fig. 3: The expression level of miR-190b, miR-584-5p, miR-452-5p, and miR-1306-5p (relative to u-48) in ER-/PR- and ER+/PR+ breast tumor samples. The results of the qRT-PCR analysis revealed that the measured expression level of miR-190b is lower in each 9 ER-/PR- samples **(A)** and is higher in each 8 ER+/PR+ samples **(B)**, in comparison with the expression levels of the other three miRNAs in those samples (The expression level of miR-452-5p was not detectable in T1, T2, T4, T8, T11, T12, T13, T14, T15, T16, and T17 samples).

Fig. 1.

A)

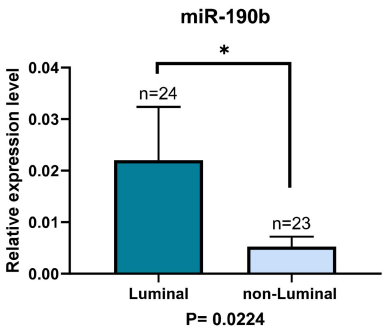
miR-190b
*
n=24
n=23
Relative expression level
0.04
0.03
0.02
0.01
0.00
Luminal
non-Luminal
P= 0.0224

B)

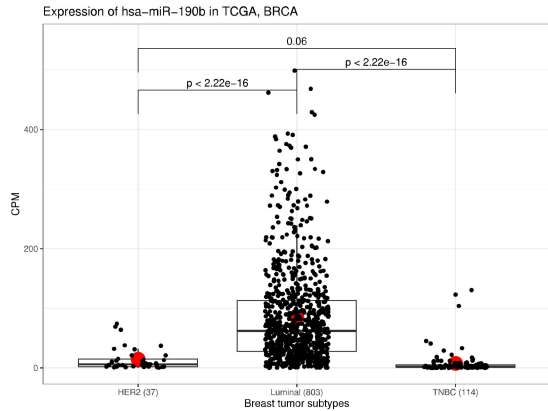
Expression of hsa−miR−190b in TCGA, BRCA
0.06
p < 2.22e−16
p < 2.22e−16
CPM
400
200
0
HER2 (37)
Luminal (803)
TNBC (114)
Breast tumor subtypes

C)

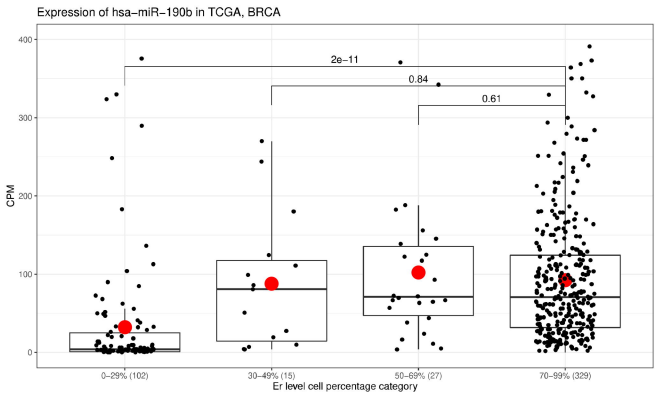
Expression of hsa−miR−190b in TCGA, BRCA
2e−11
0.84
0.61
CPM
400
300
200
100
0
0−29% (102)
30−49% (15)
50−69% (27)
70−99% (329)
Er level cell percentage category

D)

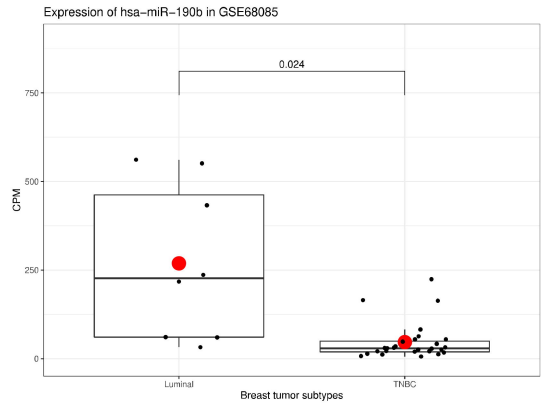
Expression of hsa−miR−190b in GSE68085
0.024
CPM
750
500
250
0
Luminal
TNBC
Breast tumor subtypes

Fig. 2.

A)

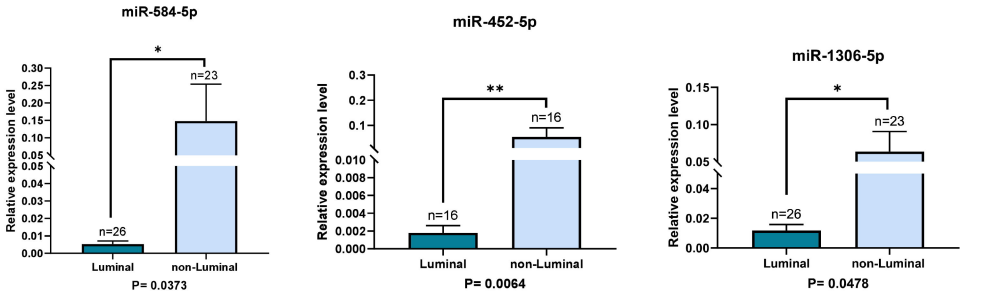
miR-584-5p
miR-452-5p
miR-1306-5p
Relative expression level
n=26
n=23
n=16
n=16
n=26
n=23
Luminal
non-Luminal
P= 0.0373
P= 0.0064
P= 0.0478

B)

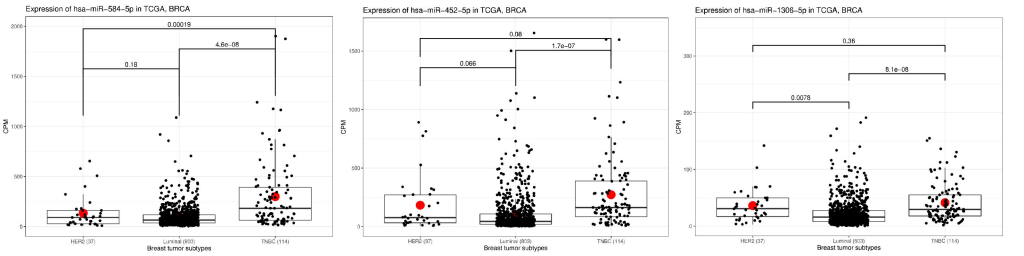
Expression of hsa-miR-584-5p in TCGA, BRCA
Expression of hsa-miR-452-5p in TCGA, BRCA
Expression of hsa-miR-1306-5p in TCGA, BRCA
CPM
Breast tumor subtypes

C)

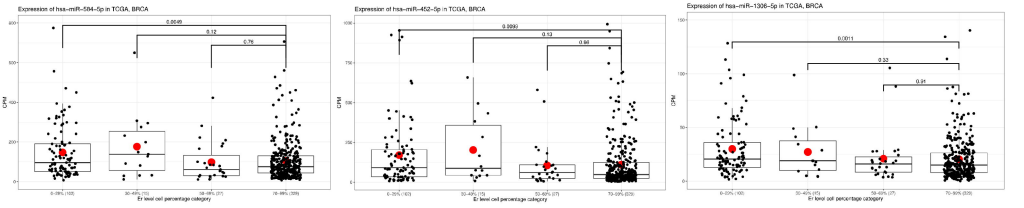
Expression of hsa-miR-584-5p in TCGA, BRCA
Expression of hsa-miR-452-5p in TCGA, BRCA
Expression of hsa-miR-1306-5p in TCGA, BRCA
CPM
Er level cell percentage category

D)

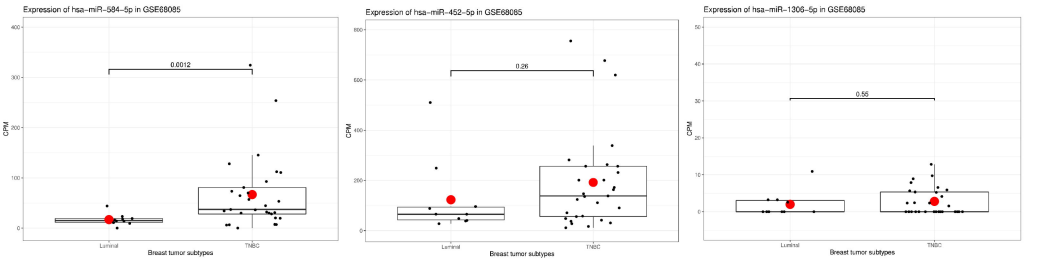
Expression of hsa-miR-584-5p in GSE68085
Expression of hsa-miR-452-5p in GSE68085
Expression of hsa-miR-1306-5p in GSE68085
CPM
Luminal
TNBC
Breast tumor subtypes

Fig. 3.

A)

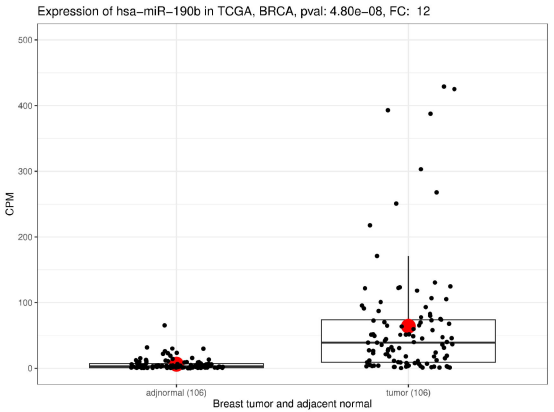
Expression of hsa−miR−190b in TCGA, BRCA, pval: 4.80e−08, FC: 12
CPM
500
400
300
200
100
0
adjnormal (106)
tumor (106)
Breast tumor and adjacent normal

B)

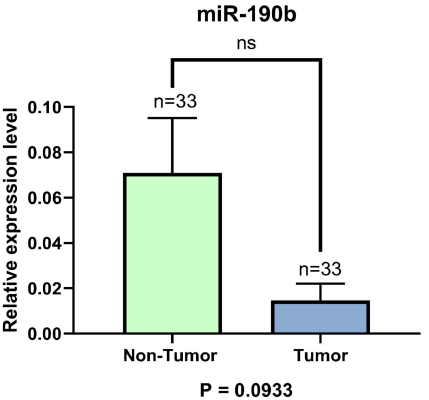
miR-190b
ns
n=33
n=33
Relative expression level
0.10
0.08
0.06
0.04
0.02
0.00
Non-Tumor
Tumor
P = 0.0933

C)

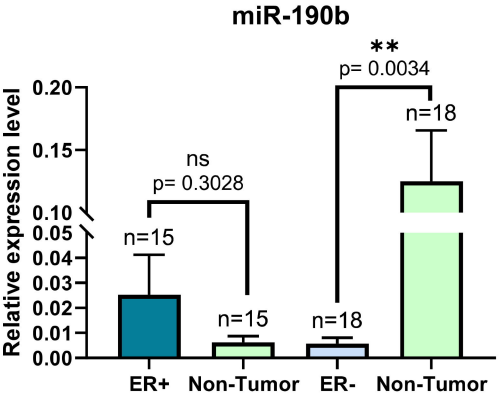
miR-190b
**
p= 0.0034
n=18
ns
p= 0.3028
n=15
n=15
n=18
Relative expression level
0.20
0.15
0.10
0.05
0.04
0.03
0.02
0.01
0.00
ER+
Non-Tumor
ER-
Non-Tumor

Fig. 4.

A)

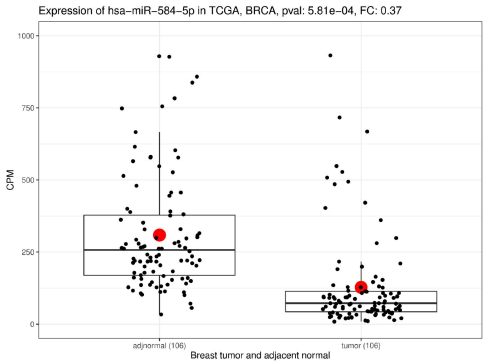
Expression of hsa−miR−584−5p in TCGA, BRCA, pval: 5.81e−04, FC: 0.37
CPM
1000
750
500
250
0
adjnormal (106)
tumor (106)
Breast tumor and adjacent normal

D)

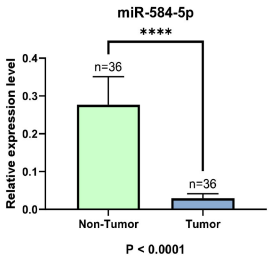
miR-584-5p
****
n=36
n=36
Relative expression level
0.4
0.3
0.2
0.1
0.0
Non-Tumor
Tumor
P < 0.0001

B)

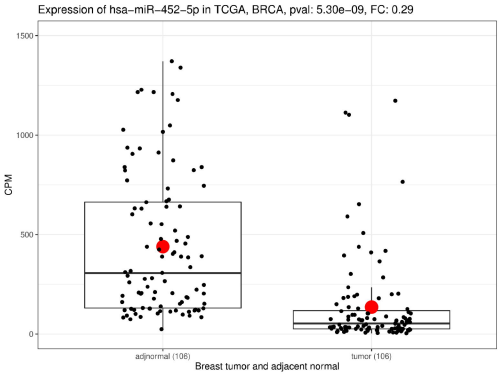
Expression of hsa−miR−452−5p in TCGA, BRCA, pval: 5.30e−09, FC: 0.29
CPM
1500
1000
500
0
adjnormal (106)
tumor (106)
Breast tumor and adjacent normal

E)

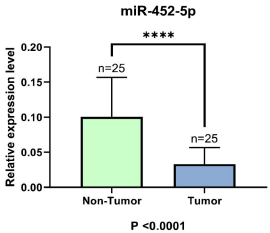
miR-452-5p
****
n=25
n=25
Relative expression level
0.20
0.15
0.10
0.05
0.00
Non-Tumor
Tumor
P <0.0001

C)

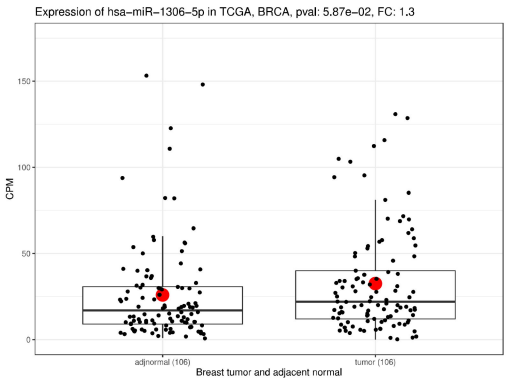
Expression of hsa−miR−1306−5p in TCGA, BRCA, pval: 5.87e−02, FC: 1.3
CPM
150
100
50
0
adjnormal (106)
tumor (106)
Breast tumor and adjacent normal

F)

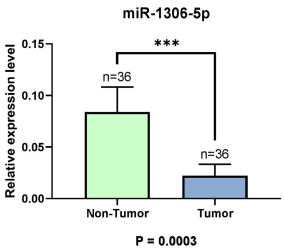
miR-1306-5p
***
n=36
n=36
Relative expression level
0.15
0.10
0.05
0.00
Non-Tumor
Tumor
P = 0.0003

A)

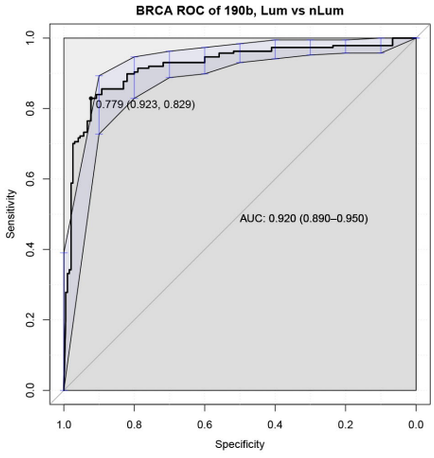
BRCA ROC of 190b, Lum vs nLum
0.779 (0.923, 0.829)
AUC: 0.920 (0.890–0.950)
Sensitivity
Specificity

B)

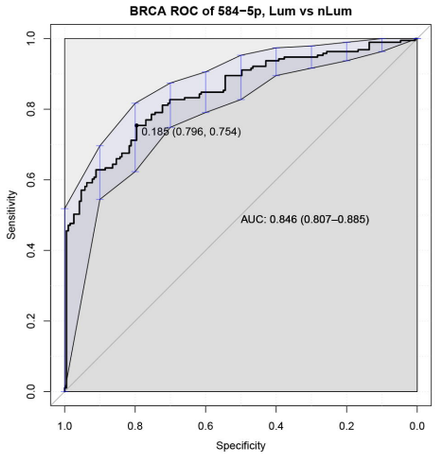
BRCA ROC of 584−5p, Lum vs nLum
0.185 (0.796, 0.754)
AUC: 0.846 (0.807–0.885)
Sensitivity
Specificity

C)

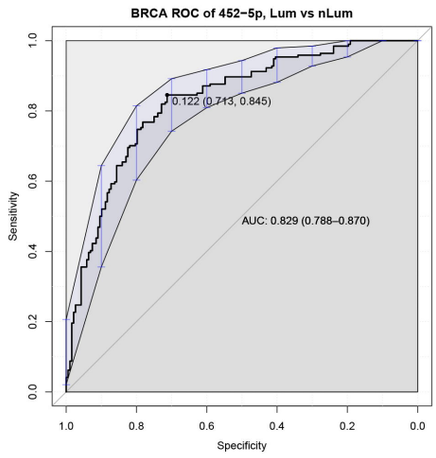
BRCA ROC of 452−5p, Lum vs nLum
0.122 (0.713, 0.845)
AUC: 0.829 (0.788–0.870)
Sensitivity
Specificity

D)

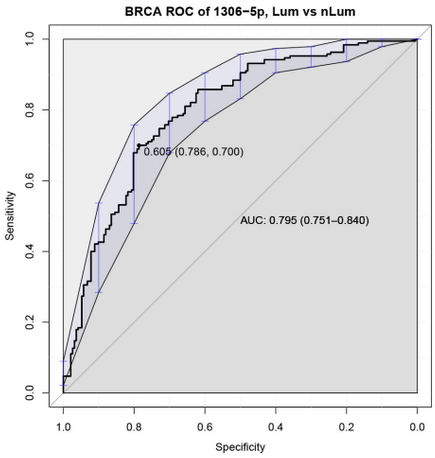
BRCA ROC of 1306−5p, Lum vs nLum
0.605 (0.786, 0.700)
AUC: 0.795 (0.751–0.840)
Sensitivity
Specificity

E)

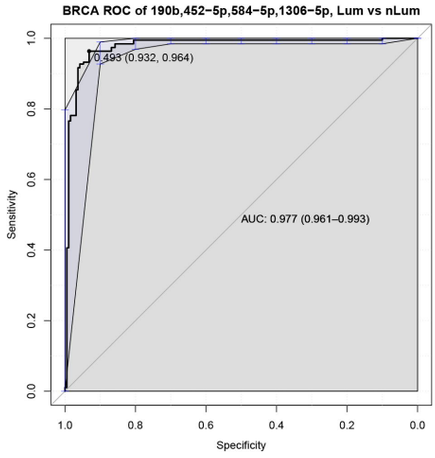
BRCA ROC of 190b,452−5p,584−5p,1306−5p, Lum vs nLum
0.493 (0.932, 0.964)
AUC: 0.977 (0.961–0.993)
Sensitivity
Specificity

F)

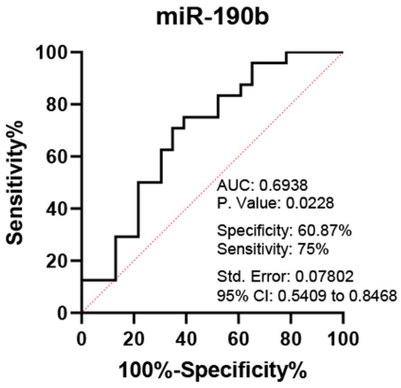
miR-190b
AUC: 0.6938
P. Value: 0.0228
Specificity: 60.87%
Sensitivity: 75%
Std. Error: 0.07802
95% CI: 0.5409 to 0.8468
Sensitivity%
100%-Specificity%

G)

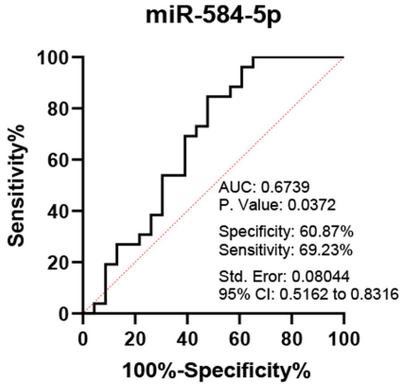
miR-584-5p
AUC: 0.6739
P. Value: 0.0372
Specificity: 60.87%
Sensitivity: 69.23%
Std. Eror: 0.08044
95% CI: 0.5162 to 0.8316
Sensitivity%
100%-Specificity%

H)

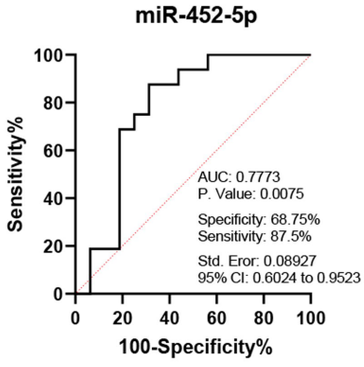
miR-452-5p
AUC: 0.7773
P. Value: 0.0075
Specificity: 68.75%
Sensitivity: 87.5%
Std. Eror: 0.08927
95% CI: 0.6024 to 0.9523
Sensitivity%
100-Specificity%

I)

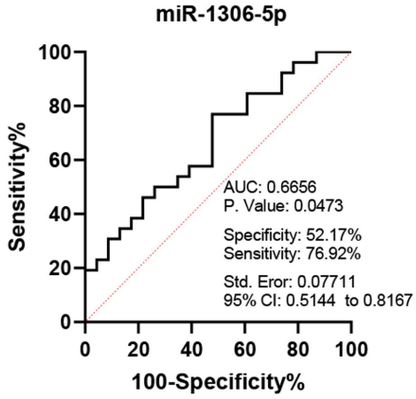
miR-1306-5p
AUC: 0.6656
P. Value: 0.0473
Specificity: 52.17%
Sensitivity: 76.92%
Std. Eror: 0.07711
95% CI: 0.5144 to 0.8167
Sensitivity%
100-Specificity%

Fig.6

A)

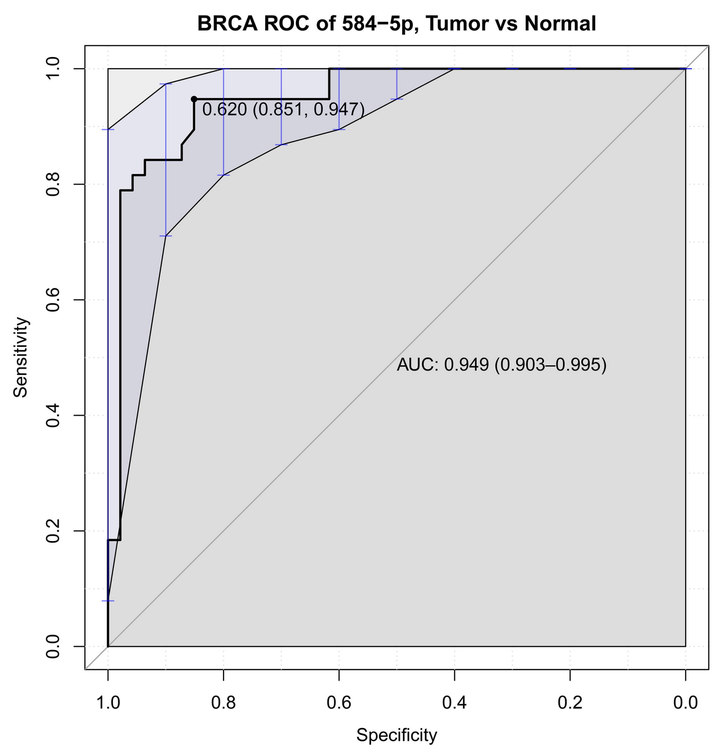

B)

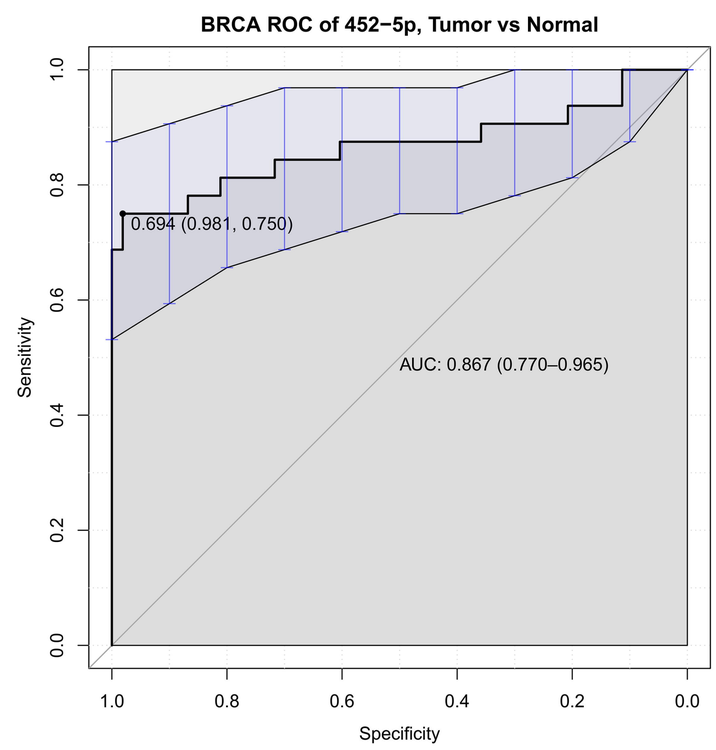

C)

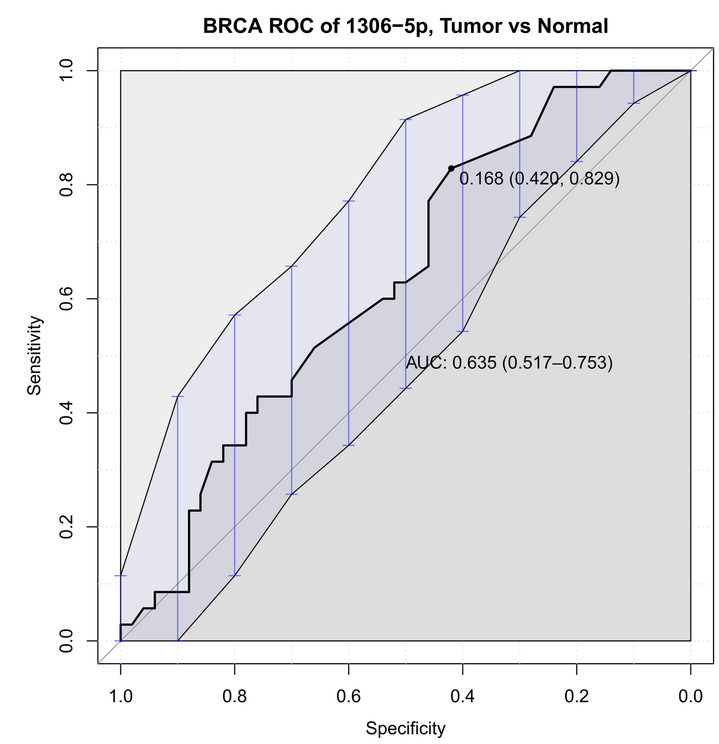

D)

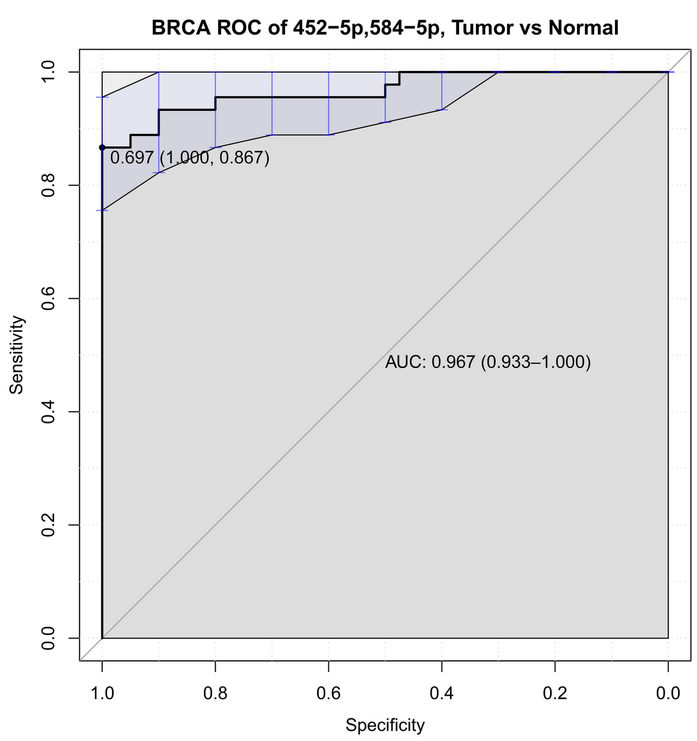

E)

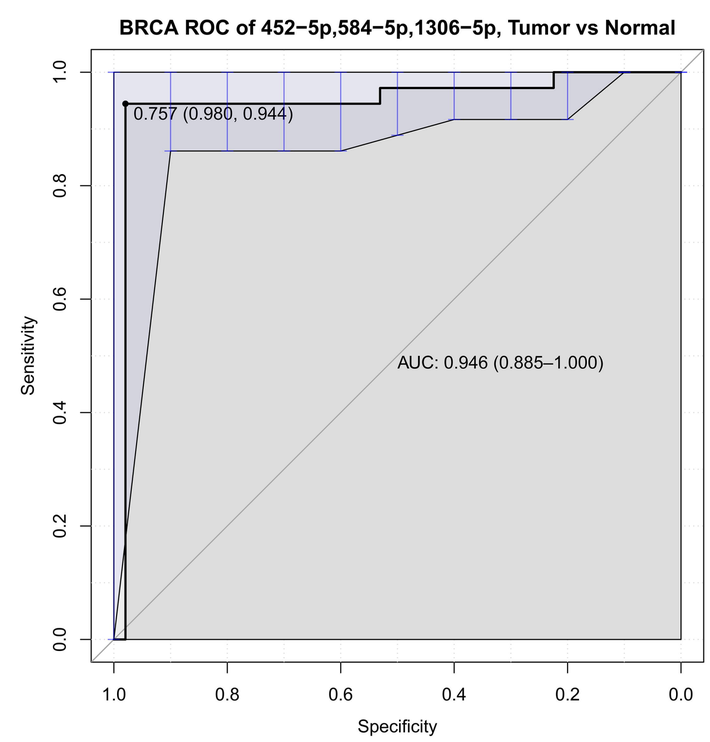

F)

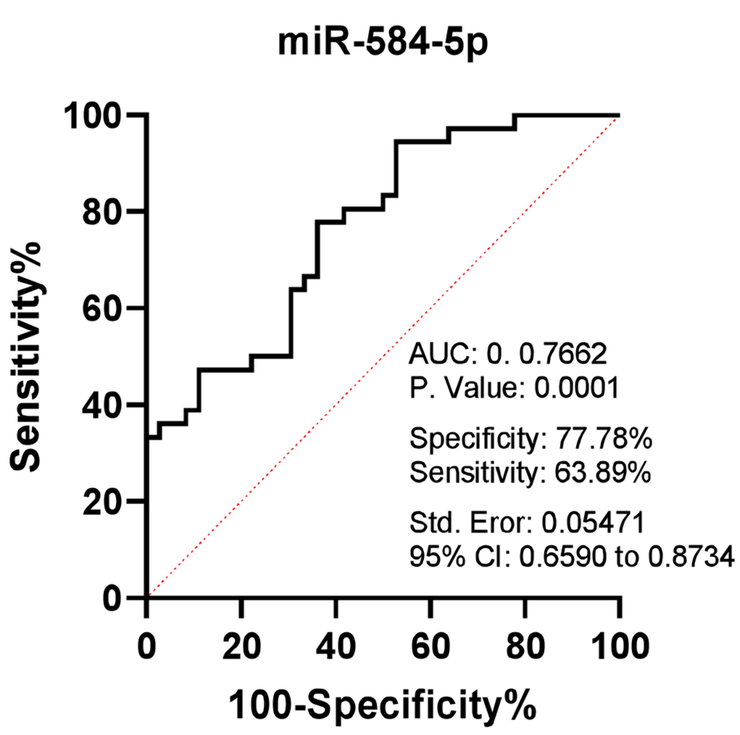

G)

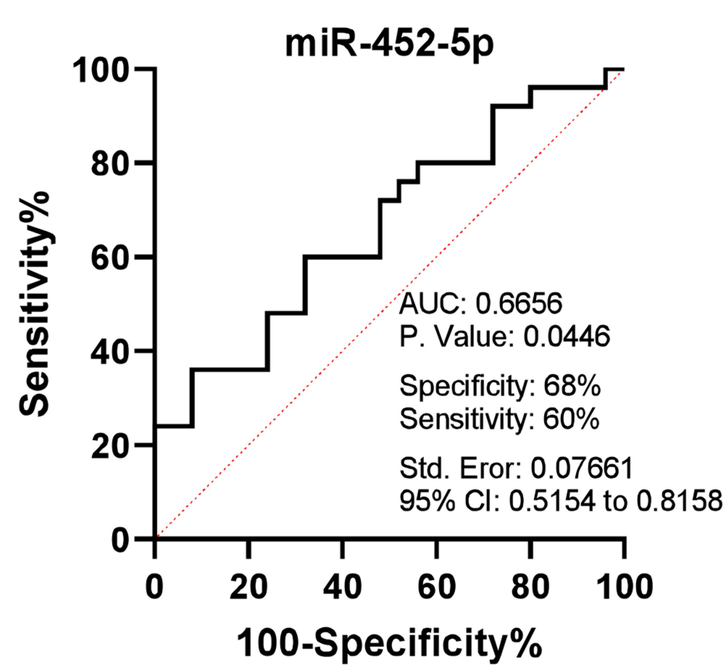
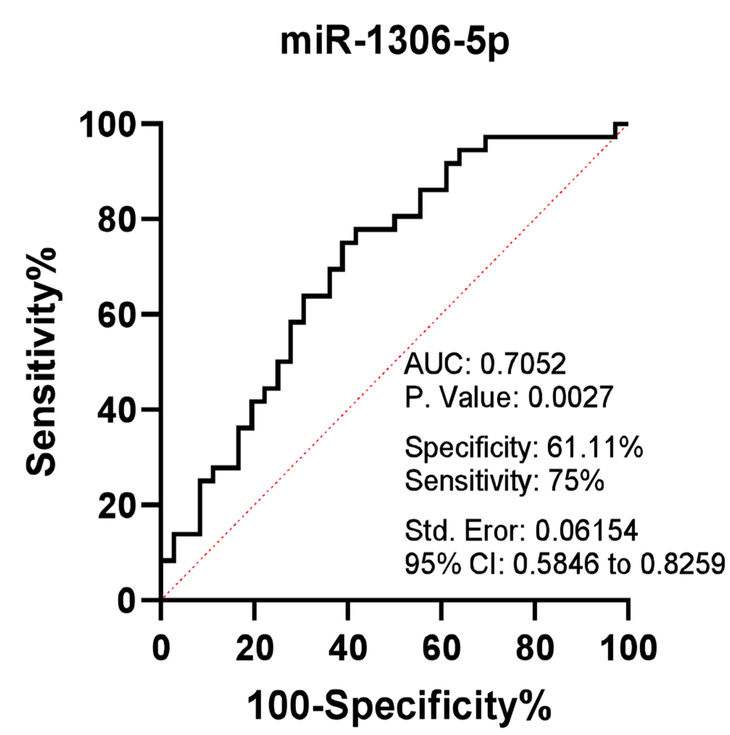
H)